

DYNAMIC OPTIMIZATION OF CHEMICALLY REACTING STAGNATION FLOWS

Laxminarayan L. Raja and Robert J. Kee
Engineering Division
Colorado School of Mines
Golden, CO 80401

Radu Serban and Linda R. Petzold
Computational Science and Engineering Program
Department of Mechanical and Environmental Engineering
University of California
Santa Barbara, CA 93106-5070

This paper presents a dynamic-optimization algorithm that can be used to minimize a generalized objective function. It is demonstrated for a chemical-vapor-deposition (CVD) process in a stagnation-flow reactor. The equations describing the chemically reacting flow are written in a transient compressible similarity form. After discretizing the spatial derivatives on a finite-volume mesh, the system becomes a set of differential-algebraic equations (DAE). The optimization algorithm is a shooting-type approach that is designed specifically to work with large nonlinear systems of DAEs. The algorithm is demonstrated using an example from the CVD growth of a thin-film YBCO high-temperature superconductor.

INTRODUCTION

The objective of this paper is to present an algorithm for planning optimal time-varying trajectories for chemical-vapor-deposition (CVD) processes and to discuss the potential benefits of doing so. The traditional strategy for CVD is to control to fixed setpoints, which are established to provide the best overall operating conditions. While this approach has generally worked well in practice, it certainly represents a highly restricted view of process control. There is potentially great value in time-varying processing conditions. However, realizing the potential benefits requires the ability to understand and control the interactions among strongly nonlinear fluid-mechanical and chemical phenomena.

What are some of the potential benefits of transient processing? In polycrystalline thin-film growth, for example, there is reason to believe that the optimal conditions for film initiation and grain nucleation are different from those that provide the best mature growth. If a single process is to operate in both regimes, there must be a strategy to transition from one to the other. In the filling of vias or trenches in semiconductor manufacture, throughput could be improved if the process itself varied throughout the course of the fill. For example higher gas pressures could be used early in the process when the features are relatively open and have low aspect ratios, with lower pressure required to maintain good step coverage as the features fill and

the aspect ratios increase. Finally, growing any functionally graded materials, such as compound semiconductors, have an obvious requirement for time-varying process conditions to produce through-thickness compositional variations in the film.

Developing optimal processing strategies requires at least four essential elements. First is a quantitative measure of the relative benefits and costs associated with any particular processing trajectory, i.e., an *objective function*. For CVD processes, the value of the film could be measured in terms of chemical composition, morphology and microstructure, and uniformity. The cost to achieve the value might be measured in terms of reagent consumption, energy costs, and throughput. A quantitative measure of both the value and the cost to achieve the value can be cast in terms of an objective function that is to be minimized by the optimal processing strategy. There may also be *constraints* that a particular process or system must obey. For example, heaters or mass-flow controllers have physical limitations on the rates at which they can respond. In some cases, film properties could also be viewed as constraints. For example, if a polycrystalline film is required, then an amorphous film simply will not do. Thus, the film structure could be cast as an inequality constraint, rather than as an increased objective function. In any case, the objective function and the constraints must be represented as functions of the *state variables* and communicated to the optimization software.

A second essential element for trajectory implementation is a means to actuate change, i.e., *controls*. Typically the controls for a CVD system are at the reactor scale, using heaters to actuate surface temperature, mass-flow controllers to vary the relative flows of precursor chemicals and carrier gases, and throttling valves to control process pressure. These controls usually appear as boundary conditions or parameters in the model.

A third essential element in planning a trajectory is to understand and predict quantitatively the effect of a control action on the objective function. Physically based computational models serve this purpose, and provide a software connection to the optimization algorithms. The models described in this paper concern stagnation-flow reactors. The chemically reacting stagnation-flow equations are developed and solved in a compressible form that is particularly well suited to transient analysis. [5] Using a method-of-lines approach, the spatial-derivative operators are approximated using finite-volume discretizations. The semi-discrete equations form a system of differential-algebraic equations (DAE).

The final element of optimal trajectory planning is the optimization algorithm itself. Here, the optimization algorithm is designed specifically to work with large systems of DAEs or ordinary differential equations (ODE) [1]. The optimal-control algorithm transforms the dynamic optimization problem for the process transients to one of parameter optimization, which is then solved using sequential quadratic programming (SQP) software [2]. This transformation is accomplished by a shooting approach where the original time domain is divided into subintervals over each of which the problem DAE's are integrated. The results presented here use a single-shooting method. However, a multiple-shooting approach is also described, which holds considerable promise for faster convergence rates and improved robustness for highly nonlinear problems.

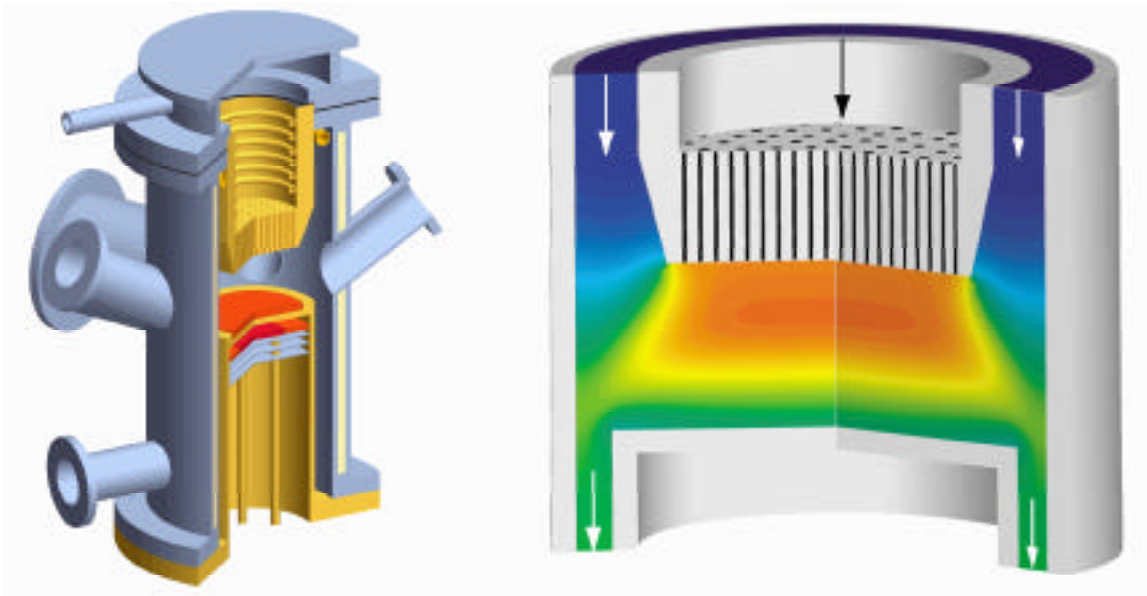


Figure 1: The sketch on the left illustrates a stagnation-flow reactor that is designed to grow YBCO thin films. The metal-organic precursors enter a heated plenum and mixing chamber at the top of the reactor. A stagnation flow region is established between a showerhead manifold and a heated wafer surface. Inert, relatively cool purge gases flow downward along the reactor walls. The exhaust gases are pumped out the bottom of the reactor chamber. The figure on the right illustrates the results of a Navier-Stokes simulation, showing in gray scales the concentration of the yttrium precursor, $Y(thd)_3$. As evidenced by the radial independence of the concentration field, the ideal stagnation flow is realized over most of the wafer surface.

Approaches similar to the one described herein have been developed by Barton, et al.[3] for optimizing industrial chemical processes and plants, and by Petzold and Zhu[4] for developing reduced chemical kinetics mechanisms using the stirred reactor configuration. This paper uses an example of a stagnation-flow reactor to demonstrate optimal control of chemically reacting flows.

STAGNATION FLOW REACTOR

An important objective in a stagnation-flow CVD reactor design is to assure that the flow field can deliver spatially uniform chemical fluxes to the deposition surface for a wide range of processing conditions. In this way, controls can be implemented to alter the growth conditions, yet still retain the necessary film uniformity. The design seeks to keep the fluid flow in a regime that approximates ideal self-similar stagnation flow over most of the wafer, thereby assuring a uniform boundary layer and deposition rate. The reactor shown in Fig. 1 achieves this objective and serves as the basis for the example problem in this paper. The reactor geometry was designed using extensive simulation.

GOVERNING EQUATIONS

The similar, axisymmetric, compressible, stagnation-flow equations are developed in Raja, et al. [5] Here the equations are summarized.

$$\frac{\partial \rho}{\partial t} + \frac{d(\rho u)}{dz} + 2\rho V = \frac{\rho}{p_{\text{ref}}} \frac{\partial p}{\partial t} - \frac{\rho}{T} \frac{\partial T}{\partial t} - \rho \bar{W} \sum_{k=1}^{K_g} \frac{1}{W_k} \frac{\partial Y_k}{\partial t} + \frac{d(\rho u)}{dz} + 2\rho V = 0 \quad (1)$$

$$\rho \frac{\partial u}{\partial t} + \rho u \frac{\partial u}{\partial z} + \frac{\partial p}{\partial z} = 0 \quad (2)$$

$$\rho \frac{\partial V}{\partial t} + \rho u \frac{dV}{dz} + \rho V^2 = -\Lambda_r + \frac{d}{dz} \left(\mu \frac{dV}{dz} \right) \quad (3)$$

$$\rho c_p \frac{\partial T}{\partial t} + \rho u c_p \frac{dT}{dz} = \frac{d}{dz} \left(\lambda \frac{dT}{dz} \right) - \sum_{k=1}^K \rho Y_k V_k c_{pk} \frac{dT}{dz} + \sum_{k=1}^K h_k W_k \dot{\omega}_k \quad (4)$$

$$\rho \frac{\partial Y_k}{\partial t} + \rho u \frac{dY_k}{dz} = -\frac{d}{dz} (\rho Y_k V_k) + W_k \dot{\omega}_k \quad (k = 1, K_g) \quad (5)$$

$$p = \rho R T \sum_{k=1}^{K_g} \frac{Y_k}{W_k}. \quad (6)$$

In these equations, the independent variables are time t and the axial coordinate z . The dependent variables are the axial velocity u , the scaled radial velocity $V = v/r$, the temperature T , and the species mass fractions Y_k . The mass density ρ is determined from the equation of state. The pressure-gradient term in the radial momentum equation $\Lambda_r = (1/r)(dp/dr)$ is an eigenvalue that must be determined in the course of the solution. The diffusion velocity of the k th species in the axial direction,

$$V_k = \frac{1}{X_k \bar{W}} \sum_{j \neq k}^K W_j D_{kj} \frac{\partial X_j}{\partial z} - \frac{D_k^T}{\rho Y_k T} \frac{1}{\partial z} \frac{\partial T}{\partial z}, \quad (7)$$

has an ordinary-multicomponent contribution and a thermal-diffusive contribution. Here, D_{kj} is the matrix of ordinary multicomponent diffusion coefficients, and D_k^T are the thermal diffusion coefficients.

The boundary conditions are specified at the inlet manifold as $u = u_{\text{in}}(t)$, $V = v/r = 0$, $T = T_{\text{in}}(t)$, and $Y_k = Y_{k,\text{in}}(t)$. In the example problem here, the control is imposed on the inlet mass fractions of the copper and barium precursors. At the deposition surface, the boundary conditions include $T = T_{\text{sur}}(t)$ and $V = 0$. The gas-phase mass fractions at the surface involve the surface chemistry. The surface states are determined from

$$\frac{dZ_k}{dt} = \frac{\dot{s}_k}{\Gamma} \quad (k = 1, \dots, K_s), \quad (8)$$

where Z_k are the surface site fractions, \dot{s}_k are the molar production rates of surface species by heterogeneous reaction, and Γ is the molar density of potentially available surface sites. The reaction mechanism for the surface and the gas phase is listed in

Table 1: Reaction Mechanism

	Reaction	A^*	E^*
G1	$Y(\text{thd})_3 + O_2 \rightarrow Y + 3(\text{thd}) + O_2$	5.9×10^{15}	27.0
G2	$Y(\text{thd})_3 \rightarrow Y + 3(\text{thd})$	2.2×10^9	34.3
G3	$Cu(\text{thd})_2 \rightarrow Cu + 2(\text{thd})$	6.03×10^9	27.06
G4	$Ba(\text{thd})_2 \rightarrow Ba + 2(\text{thd})$	2.2×10^9	34.3
G5	$4Y + 3O_2 \rightarrow 2Y_2O_3$	“fast”	
G6	$2 Ba + O_2 \rightarrow 2 BaO$	“fast”	
G7	$2 Cu + O_2 \rightarrow 2 CuO$	“fast”	
S1	$Y_2O_3 \rightarrow Y_2O_3(d)$	0.5^\dagger	
S2	$BaO \rightarrow BaO(d)$	0.5^\dagger	
S3	$CuO \rightarrow CuO(d)$	0.5^\dagger	

* Arrhenius parameters for the rate constants written in the form:

$k = A \exp(-E / RT)$. The units of A are given in terms of mols, cubic centimeters, and seconds. E is in kcal/mol.

† Sticking coefficient. The value 0.5 is simply assumed for this example

Table 1. The coupling between the gas and the surface is established through the mass-flux balance at the surface

$$\rho Y_k (u_{st} + V_k) = \dot{s}_k W_k, \quad (k = 1, \dots, K_g), \quad (9)$$

where u_{st} is the Stefan velocity and W_k are the species molar masses.

The reaction mechanism provides for gas-phase decomposition of the metal-organic precursors by oxidative reaction and by unimolecular decomposition. The rates for the yttrium and copper precursors are measured, but the product species are not. The authors are not aware of any measurements for barium decomposition. For the purpose of this work it is assumed that the barium precursor undergoes unimolecular decomposition in the gas-phase at the same rate as the yttrium precursor. This mechanism also postulates that the “growth species” are volatile metal oxides that result from gas-phase reaction. They are labeled as stable oxides, e.g. Y_2O_3 , although there is no evidence for the specific form of the oxides.

The system of partial differential equations is solved by a method-of-lines algorithm, wherein the spatial derivatives are approximated using a finite-volume discretization. In the semi-discrete form, the equations become a system of index-two DAEs. The algebraic contributions come from the pressure-curvature eigenvalue Λ_r and the discretized continuity equation at the last spatial node adjacent to the inlet manifold. With some manipulation, the equations can be reduced to an index-one system, which is solvable by DAE software such as DASSL or DASPK [6].

ALGORITHMS AND SOFTWARE FOR OPTIMAL CONTROL

The physical problem (chemically reacting stagnation flow) can be represented as a differential-algebraic equation (DAE) system

$$F(t, x, x', p, u(t)) = 0, \quad x(t_0) = x_0,$$

where x is a vector of the DAE state variables and the DAE is index one [5], [6], [7]. The initial conditions x_0 have been chosen so that they are consistent (i.e. constraints of the DAE are satisfied). The control parameters p and the vector-valued control function $u(t)$ must be determined such that the objective function

$$\int_{t_0}^{t_{\max}} \Psi(t, x(t), p, u(t)) dt \quad \text{is minimized}$$

and some additional inequality constraints

$$G(t, x(t), p, u(t)) \geq 0$$

are satisfied. (Following convention, the variable $u(t)$ is used here to represent the control function and p the control parameters. Note that earlier in the paper the variable u was used to represent a fluid velocity and p the pressure.) The optimal control function $u^*(t)$ is assumed to be continuous. In this application the DAE system is large, i.e., roughly 500 state variables. Thus, the dimension n_x of x is large. However, the dimension of the control parameters and of the representation of the control function $u(t)$ is much smaller. To represent $u(t)$ in a low-dimensional vector space, we use piecewise polynomials on $[t_0, t_{\max}]$, their coefficients being determined by the optimization. For ease of presentation we can therefore assume that the vector p contains both the parameters and these coefficients (we let n_p denote the combined number of these values) and discard the control function $u(t)$ in the remainder of this paper. Hence we consider

$$F(t, x, x', p) = 0, \quad x(t_0) = x_0, \quad (10a)$$

$$\int_{t_0}^{t_{\max}} \psi(t, x(t), p) dt \quad \text{is minimized}, \quad (10b)$$

$$g(t, x(t), p) \geq 0. \quad (10c)$$

There are a number of methods for direct discretization of this optimal control problem, Eq. 10. The *single shooting method* solves the DAEs, Eq. 10a, over the interval $[t_0, t_{\max}]$, with the set of controls p generated at each iteration by the optimization algorithm. However, in some problems single shooting can suffer from a lack of stability and robustness [8]. Moreover, it can be more difficult to maintain additional constraints and to ensure that the iterates are physical or computable. The *finite-difference method* or *collocation method* discretizes the DAEs over the interval $[t_0, t_{\max}]$ with the DAE solutions at each discrete time and the set of controls generated at each iteration by the optimization algorithm. Although this method is more robust and stable than the single shooting method, it requires the solution of an optimization problem which for a large-scale DAE system is enormous, and it does not allow for the use of adaptive DAE or (in the case that the DAE system is the result of semi-discretization of PDEs) PDE software.

The single-shooting approach has performed well for the limited number of CVD problems that we have done and the results presented in this paper use the single-shooting approach. Nevertheless, it appears that the overall efficiency and reliability can be improved with a *multiple-shooting method* and a new modification of it that exploits problem structure to reduce complexity. The single shooting can be explained

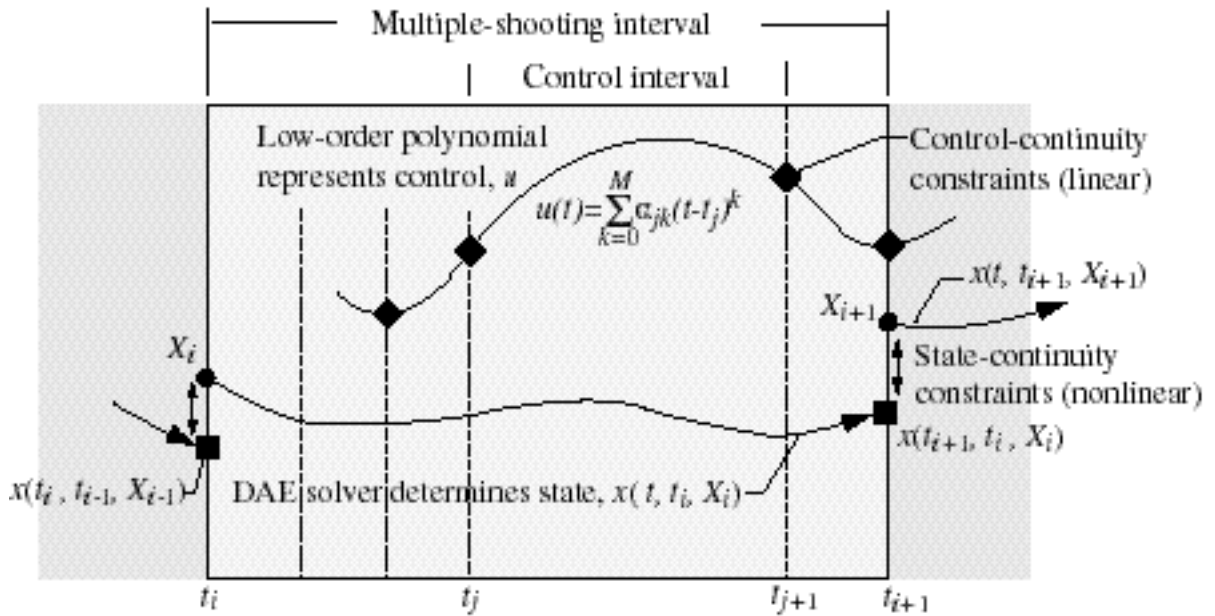


Figure 2: Illustration of the salient features of optimal control algorithm

within the context of the multiple shooting method and we are currently working on extending the CVD optimal control model to incorporate the modified multiple shooting method. In the multiple shooting method, the time interval $[t_0, t_{\max}]$ is divided into subintervals $[t_i, t_{i+1}]$ ($i = 0, \dots, N - 1$), and the differential equations, Eq. 10a, are solved separately over each subinterval. Figure 2 is an illustration of the multiple shooting subinterval. The initial conditions X_i , for the DAE solution on the subintervals are treated as parameters to be optimized along with the controls p . On each subinterval the DAE solution at time t with initial value X_i at t_i is denoted by $x(t, t_i, X_i, p)$.

DAE state continuity between subintervals is achieved via the state-continuity constraints on the optimization problem

$$C_1^{i+1}(X_i, X_{i+1}, p) := X_{i+1} - x(t_{i+1}, t_i, X_i, p) = 0.$$

For the DAE solution to be defined on each multiple-shooting subinterval, it must be provided with a set of initial values that are consistent (i.e., the initial values must satisfy the algebraic constraints in the DAE). This is not generally the case with initial values provided by methods like SQP because these methods are “infeasible” (in other words, intermediate solutions generated by the optimizer do not necessarily satisfy the above nonlinear constraints in the optimization problem although the final solution does). To begin each interval with a consistent set of initial values, we must first project the intermediate solution generated by SNOPT onto the constraints, and then solve the DAE system over the subinterval.

Additional constraints can be specified (10c) at the boundaries of the shooting intervals

$$C_3^i(X_i, p) := g(t_i, X_i, p) \geq 0, \quad C_3^N(X_N, p) := g(t_N, X_N, p) \geq 0,$$

and also at a finite number of intermediate times t_{ik} within each subinterval $[t_i, t_{i+1}]$

$$C_2^{ik}(X_i, p) := g(t_{ik}, x(t_{ik}, t_i, X_i, p), p) \geq 0.$$

In addition to the multiple-shooting subintervals of the entire time domain $[t_0, t_{\max}]$, each subinterval can be further subdivided into *control intervals* $[t_j, t_{j+1}]$ as shown in Fig. 2. The control in this interval $u_j(t, p)$ is represented as a polynomial of order M . The continuity of the controls requires two linear constraints at the control interfaces. The linear constraints enforce control continuity and differentiability along the entire time domain and are satisfied by the optimizer at all iterations. These are represented as

$$C_4^j(p) := u_j(t_j, p) - u_{j+1}(t_j, p) = 0 \quad \text{and} \quad C_5^j(p) := \frac{d}{dt}u_j(t_j, p) - \frac{d}{dt}u_{j+1}(t_j, p) = 0.$$

Following common practice, we write

$$\Phi(t) = \int_{t_0}^t \psi(\tau, x(\tau), p) d\tau,$$

which satisfies $\Phi'(t) = \psi(t, x(t), p)$, $\Phi(t_0) = 0$. This introduces another equation and variable into the differential system (10a). The discretized optimal control problem becomes

$$\underset{X_1, \dots, X_N, p}{\text{minimize}} \quad \Phi(t_{\max}) \tag{11}$$

subject to the constraints

$$C_1^{i+1}(X_i, X_{i+1}, p) = 0, \tag{12a}$$

$$C_2^{ik}(X_i, p) \geq 0, \tag{12b}$$

$$C_3^i(X_i, p) \geq 0 \quad \text{and} \quad C_3^N(X_N, p) \geq 0, \tag{12c}$$

$$C_4^j(p) = 0 \quad \text{and} \quad C_5^j(p) = 0. \tag{12d}$$

The single-shooting method, without any constraints on the DAE state variables, solves Eq. 11 along with the linear continuity constraints Eq. 12d. The parameters that are optimized include only the controls p .

This problem can be solved by an optimization code. We use a modified version of the solver SNOPT [2], which incorporates a sequential quadratic programming (SQP) method (see [9]). The SQP methods require a gradient and Jacobian matrix that are the derivatives of the objective function and constraints with respect to the optimization variables. We compute these derivatives via differential-algebraic equation (DAE) sensitivity software DASPKSO [10]. The sensitivity equations to be solved by DASPKSO are generated via the automatic differentiation software ADIFOR [11]. The basic algorithms and software for the optimal control of dynamical systems are described in detail in [1].

This basic multiple-shooting type of strategy can work very well for small-to-moderate size DAE systems, and has an additional advantage that it is inherently

parallel. However, for large-scale DAE systems there is a problem because the computational complexity grows rapidly with the dimension of the DAE system. The difficulty lies in the computation of the derivatives of the DAE state continuity constraints (12a-12b) with respect to the variables X_i . The computational complexity of the multiple shooting method for this type of problem can be modified to make use of the structure of the continuity constraints to reduce the number of sensitivity solutions which are needed to compute the derivatives. This modification results in a computational complexity that is roughly the same as that of single shooting. Details of the modified multiple shooting method are given in [12].

EXAMPLE PROBLEM

The example problem considers a stagnation-flow reactor that is designed to grow thin-film polycrystalline high-temperature superconductors of yttrium-barium-copper-oxide $\text{YBa}_2\text{Cu}_3\text{O}_{7-\delta}$. Three beta-diketonate metal-organic compounds, $\text{Y}(\text{thd})_3$, $\text{Ba}(\text{thd})_2$, and $\text{Cu}(\text{thd})_2$ carry the metals into reactor and are dilute in O_2 . For the example, a wafer-surface temperature variation is imposed. Such a transient process might be designed to promote film nucleation at one temperature, then transition to another temperature that is preferable for mature film growth. Throughout growth it is critical to maintain the precise ratios of the metal atom fluxes to the substrate so that the film preserves the correct stoichiometry. If the metal incorporation is permitted to vary very much, either a non-superconducting material will grow or phase-segregated non-superconducting oxides will appear. Either alternative is unacceptable. Thus, as the surface temperature changes, the precursor flow rate must be varied to compensate for the temperature-dependent effects in the flow field and the chemistry and to maintain the correct film composition. Planning these trajectories is the objective of the example problem.

The metal flux variations are a consequence of gas-phase transport and chemistry effects. As the surface temperature rises, the homogeneous reaction rates in the gas-phase boundary layer increases, accelerating the decomposition of the precursors. Also, variations in the gas-phase temperature gradients alters the molecular diffusion of species, especially by thermal diffusion for the heavy precursor compounds. Finally, the surface reaction rates depend on the surface temperature. Thus, as the temperature varies, the net gas-phase fluxes of the metal-containing compounds to the surface can vary greatly and nonlinearly.

The above effects are illustrated in Fig. 3. Here, two steady-state gas-phase species profiles are shown for the same reactor conditions but with different substrate temperatures. The precursor mole fractions at the inlet are such that the metal deposition fluxes are in the correct stoichiometric ratios: $\text{Y/Ba/Cu}:1/2/3$, at the substrate temperature of 1100 K. For a low substrate temperature of 800 K the barium precursor shows the least decomposition while the copper precursor shows the most decomposition. Clearly, the deposition of the growth species (metal-oxides) is limited by the transport of the oxides in the boundary layer. However, since the abundance of the different metal-oxides at the boundary-layer edge varies due to different precursor decomposition rates, the flux of metals to the substrate depends primarily on the gas-phase precursor decomposition rates. The barium deposition flux on the sub-

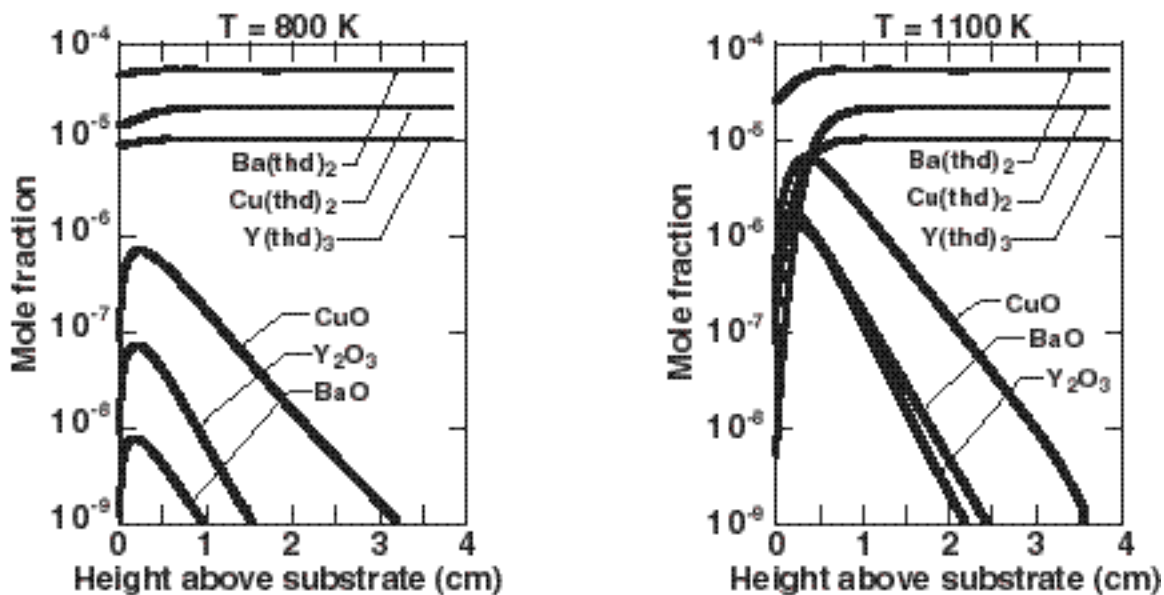


Figure 3: Gas-phase species profiles at two different substrate temperatures.

strate is thus about an order of magnitude less than the yttrium deposition flux. At a substrate temperature of 1100 K the barium precursor decomposition is comparable to the yttrium precursor and the corresponding deposition fluxes are comparable for the two metals. A process designed to produce stoichiometric films at 1100 K will produce films that are deficient in barium at lower temperatures. Thus, temporal surface-temperature variations in a process without precursor control can have deleterious consequences on film quality.

This paper discusses control of only the $\text{Ba}(\text{thd})_2$ precursor with the yttrium precursor inlet conditions remaining fixed. Since all precursors are very dilute (mole fractions $< 10^{-4}$) and the gas-phase chemistries for the three precursors are independent of each other, the control of each precursor can be studied separately. The temperature at the surface is increased from 900 K to about 1100 K in 200 seconds along an exponential trajectory as shown in Fig. 4. The initial precursor flow rates are such that stoichiometric films are produced at 900 K. The time domain of 200 seconds is subdivided into 5 control intervals and the control function for the barium precursor at the inlet is represented by a quadratic approximation in each control interval. The quadratic approximation is the lowest order polynomial on which the linear continuity and differentiability constraints can be imposed while still being able to represent a sufficiently complicated control over the time domain. This results in 15 parameters for optimization and 8 linear control continuity constraints. The objective function used in this problem seeks to maintain the barium-to-yttrium flux ratio at two is as follows

$$\psi(t, x(t), p) = \left(2 - \frac{\dot{s}_{Ba}}{\dot{s}_Y} \right)^2,$$

where the surface mole fluxes of barium atoms and yttrium atoms are given by \dot{s}_{Ba} and \dot{s}_Y , respectively. While the above objective function represents a simple measure of the quality of the film, one could certainly "design" more complicated functions

that penalize barium fluxes that lead to barium rich films to a greater extent than fluxes that lead to barium deficient films. This is certainly an important factor in obtaining good quality superconducting films. One could also include other aspects of the optimization problem such as precursor utilization in the objective function.

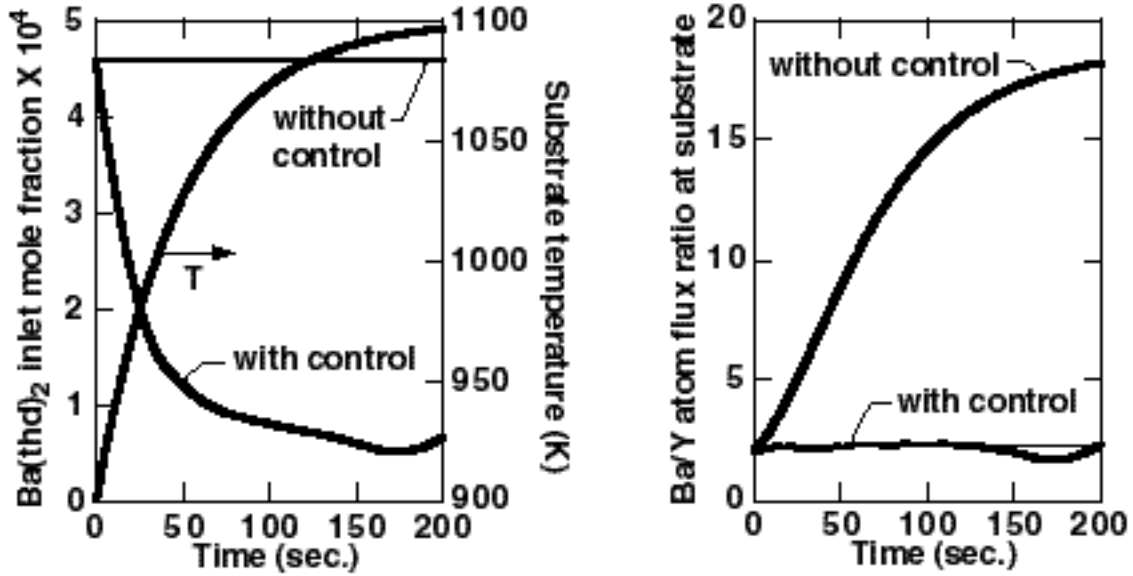


Figure 4: The panel on the left shows the trajectories of the specified surface temperature, and the $\text{Ba}(\text{thd})_2$ inlet mole fractions, with and without control. The plot on the right shows the Ba/Y atom-flux ratios that are incorporated into the film, with and without control.

The optimal solution for barium precursor control is shown in Fig. 4. The barium inlet mole fraction drops sharply from its initial value in the first 50 seconds of the transient. This is followed by a relatively shallow decrease in the inlet flow mole fractions for the rest of the transient. Figure 4 also shows the barium-to-yttrium atom flux ratios at the substrate for the transient with barium precursor control and without control. Clearly, the case without control leads to a large increase in the fraction of barium to yttrium atom fluxes deposited on the substrate as the substrate temperature is increased. When control is implemented on the barium precursor at the inlet, the barium to yttrium atom fluxes remain close to the stoichiometric ratio of two throughout the transient. The copper precursor inlet conditions can be optimized similarly.

SUMMARY

Time-varying chemical-vapor-deposition processing is an alternative that potentially offers significant advantages over traditional approaches. Optimal trajectory planning provides an important simulation tool to assist development of such processes. The overall strategy is to design path-following processes that minimize a specified cost function. The algorithm presented here is implemented in a general setting that accommodates physical models that can be written as systems of differential-algebraic equations, including those coming from the discretization of partial differential equations. The method and software are general, with potentially wide application.

ACKNOWLEDGEMENTS

This work was supported by NSF and DARPA within the Virtual Integrated Processing program. The reactor illustrated in Fig. 1 was designed jointly with Prof. David Goodwin and colleagues at the California Institute of Technology, where the reactor is located and operated.

REFERENCES

1. L. Petzold, J. B. Rosen, P. E. Gill, L. O. Jay and K. Park, *Numerical Optimal Control of Parabolic PDEs using DASOPT*, Large Scale Optimization with Applications, Part II: Optimal Design and Control, Eds. L. Biegler, T. Coleman, A. Conn and F. Santosa, IMA Volumes in Mathematics and its Applications, Vol. 93, p. 271, (1997).
2. P. E. Gill, W. Murray, and M. A. Saunders, *SNOPT: An SQP algorithm for large-scale constrained optimization*, Numerical Analysis Report 97-2, Department of Mathematics, University of California, San Diego, La Jolla, CA, (1997).
3. P.I. Barton, R.J. Allgor, W.F. Feehery, and S. Galan, *Ind. Eng. Chem. Res.*, **37**, 966 (1998).
4. L.R. Petzold and W. Zhu, *AIChE J.*, submitted (1998).
5. L.L. Raja, R.J. Kee, and L.R. Petzold, "Simulation of the Transient, Compressible, Gas-Dynamic, Behavior of Catalytic-Combustion Ignition in Stagnation Flows," to appear, 27th Symposium (International) on Combustion, The Combustion Institute, Pittsburg, PA, (1998).
6. K. E. Brenan, S. L. Campbell, and L. R. Petzold, *Numerical Solution of Initial-Value Problems in Differential-Algebraic Equations*, 2nd ed., SIAM, Philadelphia, (1995).
7. U. M. Ascher and L. R. Petzold, *Computer Methods for Ordinary Differential Equations and Differential-Algebraic Equations*, SIAM, (1998).
8. U. M. Ascher, R. M. M. Mattheij, and R. D. Russell, *Numerical Solution of Boundary Value Problems for Ordinary Differential Equations*, SIAM, Philadelphia, PA, (1995).
9. P. E. Gill, W. Murray, and M. H. Wright, *Practical Optimization*, Academic Press, New York, (1981).
10. T. Maly and L. R. Petzold, *Applied Numerical Mathematics*, **20**, 57 (1996).
11. C. Bischof, A. Carle, G. Corliss, A. Griewank, and P. Hovland, *Scientific Programming*, **1**, 11 (1992).
12. P. E. Gill, L. O. Jay, M. W. Leonard, L. R. Petzold and V. Sharma, *An SQP Method for the Optimal Control of Large-Scale Dynamical Systems*, submitted, (1998).

References

- [1] L. Petzold, J. B. Rosen, P. E. Gill, L. O. Jay and K. Park, *Numerical Optimal Control of Parabolic PDEs using DASOPT*, Large Scale Optimization with Applications, Part II: Optimal Design and Control, Eds. L. Biegler, T. Coleman, A. Conn and F. Santosa, IMA Volumes in Mathematics and its Applications, Vol. 93, (1997), pp. 271-300.
- [2] P. E. Gill, W. Murray, and M. A. Saunders, *SNOPT: An SQP algorithm for large-scale constrained optimization*, Numerical Analysis Report 97-2, Department of Mathematics, University of California, San Diego, La Jolla, CA, 1997.
- [3] P.I. Barton, R.J. Allgor, W.F. Feehery, and S. Galan, *Ind. Eng. Chem. Res.*, **37**, 1998, pp. 966-981.
- [4] L.R. Petzold and W. Zhu, *AIChE J.*, submitted (1998).
- [5] L.L. Raja, R.J. Kee, and L.R. Petzold, "Simulation of the Transient, Compressible, Gas-Dynamic, Behavior of Catalytic-Combustion Ignition in Stagnation Flows," 27th Symposium (International) on Combustion, Boulder, CO, Aug. 2-7, 1998.
- [6] K. E. Brenan, S. L. Campbell, and L. R. Petzold, *Numerical Solution of Initial-Value Problems in Differential-Algebraic Equations*, SIAM Publications, Philadelphia, second ed., 1995. ISBN 0-89871-353-6.
- [7] U. M. Ascher and L. R. Petzold, *Computer Methods for Ordinary Differential Equations and Differential-Algebraic Equations*, SIAM, 1998.
- [8] U. M. Ascher, R. M. M. Mattheij, and R. D. Russell, *Numerical Solution of Boundary Value Problems for Ordinary Differential Equations*, Society for Industrial and Applied Mathematics (SIAM) Publications, Philadelphia, PA, 1995. ISBN 0-89871-354-4.
- [9] P. E. Gill, W. Murray, and M. H. Wright, *Practical Optimization*, Academic Press, London and New York, 1981. ISBN 0-12-283952-8.
- [10] T. Maly and L. R. Petzold, *Numerical methods and software for sensitivity analysis of differential-algebraic systems*, Applied Numerical Mathematics 20 (1996), pp. 57-79.
- [11] C. Bischof, A. Carle, G. Corliss, A. Griewank, and P. Hovland, *ADIFOR—generating derivative codes from Fortran programs*, Scientific Programming, 1 (1992), pp. 11-29.
- [12] P. E. Gill, L. O. Jay, M. W. Leonard, L. R. Petzold and V. Sharma, *An SQP Method for the Optimal Control of Large-Scale Dynamical Systems*, submitted, 1998.